Top-spin analysis of new scalar and tensor interactions in e^+e^- collisions with beam polarization

B. Ananthanarayan,[1] Monalisa Patra,[1] and Saurabh D. Rindani[2]

[1]*Centre for High Energy Physics, Indian Institute of Science, Bangalore 560 012, India*

[2]*Theoretical Physics Division, Physical Research Laboratory, Navrangpura, Ahmedabad 380 009, India*

(Received 30 July 2010; revised manuscript received 7 December 2010; published 21 January 2011)

We utilize top polarization in the process $e^+e^- \to t\bar{t}$ at the International Linear Collider (ILC) with transverse beam polarization to probe interactions of the scalar and tensor type beyond the standard model and to disentangle their individual contributions. Ninety percent confidence level limits on the interactions with realistic integrated luminosity are presented and are found to improve by an order of magnitude compared to the case when the spin of the top quark is not measured. Sensitivities of the order of a few times 10^{-3} TeV^{-2} for real and imaginary parts of both scalar and tensor couplings at $\sqrt{s} = 500$ and 800 GeV with an integrated luminosity of 500 fb^{-1} and completely polarized beams are shown to be possible. A powerful model-independent framework for inclusive measurements is employed to describe the spin-momentum correlations, and their C, P, and T properties are presented in a technical appendix.

DOI: 10.1103/PhysRevD.83.016010 PACS numbers: 11.30.Er, 13.66.Jn, 13.88.+e

I. INTRODUCTION

At the planned International Linear Collider (ILC) [1], $e^+e^- \to t\bar{t}$ is a process that will be studied at great precision to validate the standard model (SM) and to look for deviations from it. The process is of continued current interest, see e.g., Ref. [2] and references therein. The availability of beam polarization will significantly enhance the sensitivity to new physics (NP), provided the electron and positron beams have transverse polarization (TP) or longitudinal polarization, each complementing the other, with distinct prospects of obtaining a very high degree of polarization for both beams [3].

One fruitful approach is to undertake a model-independent analysis which may be performed by introducing higher dimensional operators consistent with gauge invariance. For an important early paper on the subject, see Ref. [4]. In the context of top pair production, the relevant higher dimensional operators are listed in Ref. [5] and references therein. In this work, we will confine ourselves to NP associated only with scalar and tensor type operators which cannot be probed at linear order unless TP is available. They are parametrized in terms of operators denoted by S_{RR} and T_{RR} in Ref. [5], which will hereafter be denoted by S and T, respectively. In a recent work [6], it was shown that in the presence of TP, if only cross sections were to be measured, azimuthal asymmetries would involve the linear combination given by

$$S + \frac{2c_A^t c_V^e}{c_V^t c_A^e} T, \tag{1}$$

where c_V^f and c_A^f, $f = e, t$ are the vector and axial-vector couplings of the Z to the electron and the top-quark, respectively, and will be explicitly given later. Therefore, it becomes important to pose the question of how these operators can be disentangled. The aim of the present work is to address this question and to demonstrate that measurement of the top-quark spin can indeed allow one to disentangle them. Indeed, this work is also motivated by the fact that it may be possible now to measure the top spin accurately, see, e.g., Ref. [7]. Also, it has been recently pointed out that top polarization can be measured reliably from decay charged-lepton angular distributions without errors arising from the tbW couplings [8].

To meet the ends described above, we have evaluated the beam-polarization dependent differential cross sections, and examined the polarization of t or $\bar{t}$. We have checked our *ab initio* evaluation of the cross sections with the results from the explicit helicity amplitudes provided by Grzadkowski [5] combined with the general framework for inclusion of TP provided in Ref. [9]. We have also carried out independent checks on the helicity amplitudes.

We will, finally, explore the reach of the ILC by defining suitable observables and asymmetries. Turning to the numerical implications of our work, we find surprisingly that the top-spin resolution allows us to probe the NP at a level an order of magnitude better than the reach reported in [6]. In spirit, therefore, this work is a natural completion of the prior work on $t\bar{t}$ production, and that of our work on inclusive processes with only momentum structure functions, thereby providing a systematic contribution to the physics program at the ILC with polarized beams.

In order to understand the formal structure of the terms in the distributions, we consider them in detail and isolate the spin-independent and spin-dependent parts of the cross section and present the results in a technical appendix. The former have been interpreted in terms of momentum structure functions arising in the treatment of the inclusive process framework of the type considered recently by us in [10], which relies on an analysis of:

$$e^+ + e^- \to h(p) + X \tag{2}$$

where h is the observed final state particle whose momentum p is measured, and X here and elsewhere refers to

an inclusive state. Furthermore, it was shown even an exclusive process such as $t\bar{t}$ production can be included in the framework of the general inclusive process [10]. Also in Ref. [11], the two-particle inclusive process

$$e^+ + e^- \to h_1(p_1) + h_2(p_2) + X \tag{3}$$

where $h_{1,2}$ are the observed final state particles whose momenta $p_{1,2}$ are measured, was considered. The above can be generalized as in the work of [12] to

$$e^+ + e^- \to h(p, s) + X \tag{4}$$

where p, s stand, respectively, for the momentum and spin of the observed particle h in the final state. However, this was not performed explicitly in [11]. The present work gives us an opportunity to do so in the context of the process at hand, thus providing a concrete illustration. The C, P, and T properties of the operators will be considered, and those of the structure functions separately so that the two frameworks can be related to one another. Furthermore, one may obtain insights into discrete symmetries of NP contributions from the nature of spin-momentum correlations. Important insights based on general inclusive processes have enriched the analysis of processes such as $Z\gamma$ production [13–15], and Zh production [16,17].

The scheme of this paper is as follows: In Sec. II, we will recall the main features of the framework where NP is introduced in terms of effective four-Fermi interactions. In Sec. III, we will consider the cross sections for $e^+e^- \to t\bar{t}$ in the presence of four-Fermi NP interactions. In Sec. IV, we consider applications using realistic luminosity and degrees of polarization at typical ILC energies of 500 and 800 GeV and obtain the 90% confidence level (CL) limits that can be placed on the NP operators by constructing suitable asymmetries. We note here that this is in an idealized situation, where a realistic measurement would produce somewhat weaker conclusions which we have not attempted to assess here. In Sec. V, we turn to the important question of realizing the proposal in terms of an actual experimental measurement. In Sec. VI, we provide a thorough discussion of the various features emerging from our investigations and present our conclusions. In the Appendix, we interpret the results obtained in the preceding section in terms of momentum and spin structure functions. The corresponding properties under the discrete symmetries C, P, and T are discussed.

II. EFFECTIVE OPERATORS AND FOUR-FERMI INTERACTION

The theoretical framework that we consider is one of the SM augmented with four-Fermi interaction that captures the effect of all the NP. In particular, for the process $e^+e^- \to t\bar{t}$, the tree level operators which will contribute are (see Ref. [6] and references therein).

$$\begin{aligned}
\mathcal{O}_{\ell q}^{(1)} &= \tfrac{1}{2}(\bar{\ell}\gamma_\mu \ell)(\bar{q}\gamma^\mu q), \\
\mathcal{O}_{\ell q}^{(3)} &= \tfrac{1}{2}(\bar{\ell}\gamma_\mu \tau^I \ell)(\bar{q}\gamma^\mu \tau^I q), \\
\mathcal{O}_{eu} &= \tfrac{1}{2}(\bar{e}\gamma_\mu e)(\bar{u}\gamma_\mu u), \\
\mathcal{O}_{\ell u} &= (\bar{\ell}u)(\bar{u}\ell), \\
\mathcal{O}_{qe} &= (\bar{q}e)(\bar{e}q), \\
\mathcal{O}_{\ell q} &= (\bar{\ell}e)\epsilon(\bar{q}u), \\
\mathcal{O}_{\ell q'} &= (\bar{\ell}u)\epsilon(\bar{q}e),
\end{aligned} \tag{5}$$

where l, q denote, respectively, the left-handed electroweak $SU(2)$ lepton and quark doublets, and e and u denote $SU(2)$ singlet charged-lepton and up-quark right-handed fields. τ^I $(I = 1, 2, 3)$ are the Pauli matrices, and ϵ is the 2×2 antisymmetric matrix, $\epsilon_{12} = -\epsilon_{21} = 1$, and generation indices are suppressed. Given the above operators, the Lagrangian which we will use is:

$$\mathcal{L} = \mathcal{L}^{\rm SM} + \frac{1}{\Lambda^2}\sum_i (\alpha_i \mathcal{O}_i + \text{H.c.}), \tag{6}$$

where α's are the coefficients which parametrize nonstandard interactions. The NP four-Fermi operators contained in the Lagrangian after Fierz transformation takes the form

$$\mathcal{L}^{4F} = \sum_{i,j=L,R}\Big[S_{ij}(\bar{e}P_i e)(\bar{t}P_j t) + T_{ij}\Big(\bar{e}\frac{\sigma_{\mu\nu}}{\sqrt{2}}P_i e\Big) \times \Big(\bar{t}\frac{\sigma^{\mu\nu}}{\sqrt{2}}P_j t\Big)\Big] \tag{7}$$

with the coefficients satisfying the following constraints:

$$\begin{aligned}
S \equiv S_{RR} = S_{LL}^*, \qquad S_{LR} = S_{RL} = 0, \\
T \equiv T_{RR} = T_{LL}^*, \qquad T_{LR} = T_{RL} = 0.
\end{aligned} \tag{8}$$

In (7), $P_{L,R}$ are, respectively, the left- and right-chirality projection matrices and the correspondence between the α_i and the $S(T)_{ij}$ may be read off from [5]. It may be recalled here that a significant discussion was provided in Ref. [6] on the scale of the operators that can arise from considerations of naturalness as well as constraints arising from such considerations as the electron electric and magnetic dipole moments.

III. DISTRIBUTIONS IN THE PRESENCE OF POLARIZATION

We consider the process $e^+e^- \to t\bar{t}$ for the cases when the spin of the top quark is measured, and the spins of the $\bar{t}$ are summed over, and vice-versa. We wish to examine the CP-violating as well as conserving contributions in the interference of the SM amplitude with the scalar and tensor four-Fermi amplitudes. We will take the electron TP to be 100% and along the positive or negative x axis, and the positron polarization to be 100%, parallel or antiparallel to the electron polarization. The z axis is chosen along the direction of the e^-. The differential cross sections for $e^+e^- \to t\bar{t}$, with the superscripts denoting the respective signs of the e^- and e^+ TP retaining the new couplings to linear order only, are:

$$\frac{d\sigma^{\pm\pm}}{d\Omega} = \frac{d\sigma^{\pm\pm}_{\rm SM}}{d\Omega} \pm \frac{h\alpha\beta}{\pi s^2}\left[\frac{s^{3/2}}{2} m_t \sin\theta\left(\mathrm{Re}T\cos\phi - \frac{1}{2}z'(\mathrm{Im}S - 2\beta\mathrm{Im}T\cos\theta)\sin\phi\right)\right]$$
$$\pm \frac{\alpha\beta}{4\pi s(s-M_z^2)}\Big[-3h\beta m_t c_A^t c_A^e \cos\theta\sin\theta\cos\phi s^{3/2}\mathrm{Re}T + \frac{3}{2}m_t s^{3/2}\sin\theta\{(\beta c_A^e c_V^t \mathrm{Re}S + 2c_V^e(\beta c_A^t - hc_V^t)\mathrm{Re}T)$$
$$\times\cos\phi + z' h c_V^e c_V^t(\mathrm{Im}S - 2\beta\mathrm{Im}T\cos\theta)\sin\phi\}\Big] \tag{9}$$

and

$$\frac{d\sigma^{\pm\mp}}{d\Omega} = \frac{d\sigma^{\pm\mp}_{\rm SM}}{d\Omega} \mp \frac{h\alpha\beta}{\pi s^2}\left[\frac{s^{3/2}}{2} m_t \sin\theta\left(\mathrm{Im}T\sin\phi - \frac{1}{2}z'(\mathrm{Re}S - 2\beta\mathrm{Re}T\cos\theta)\cos\phi\right)\right]$$
$$\pm \frac{\alpha\beta}{4\pi s(s-M_z^2)}\Big[3h\beta m_t c_A^t c_A^e \cos\theta\sin\theta\sin\phi s^{3/2}\mathrm{Im}T - \frac{3}{2}m_t s^{3/2}\sin\theta\{(\beta c_A^e c_V^t \mathrm{Im}S + 2c_V^e(\beta c_A^t - hc_V^t)\mathrm{Im}T)\sin\phi$$
$$+ z' h c_V^e c_V^t(\mathrm{Re}S - 2\beta\mathrm{Re}T\cos\theta)\cos\phi\}\Big] \tag{10}$$

where

$$\frac{d\sigma^{+\pm}_{\rm SM}}{d\Omega} = \frac{d\sigma^{-\mp}_{\rm SM}}{d\Omega} = \frac{3\alpha^2\beta}{4s}\Big[\frac{4}{9}\Big\{\frac{1}{2}(1+\cos^2\theta) + \frac{2m_t^2}{s}\sin^2\theta \pm \frac{1}{2}\beta^2\sin^2\theta\cos2\phi\Big\}$$
$$-\frac{s}{s-M_Z^2}\frac{4}{3}\Big\{\frac{1}{2}c_V^e(c_V^t - h\beta c_A^t)(1+\cos^2\theta) + \frac{2m_t^2}{s}c_V^e c_V^t\sin^2\theta + c_A^e(\beta c_A^t - hc_V^t)\cos\theta$$
$$\pm\frac{1}{2}\beta c_V^e(\beta c_V^t - hc_A^t)\sin^2\theta\cos2\phi\Big\} + \frac{s^2}{(s-M_Z^2)^2}\Big\{\frac{1}{2}(c_A^{e^2} + c_V^{e^2})\Big((c_V^t - h\beta c_A^t)^2(1+\cos^2\theta) + \frac{4m_t^2}{s}c_V^{t^2}\sin^2\theta\Big)$$
$$-2hc_A^e c_V^e(c_V^{t^2} + \beta^2 c_A^{t^2})\cos\theta + 4\beta\cos\theta c_A^e c_V^e c_A^t c_V^t \pm \frac{1}{2}(c_V^{e^2} - c_A^{e^2})(\beta^2(c_A^{t^2} + c_V^{t^2}) - 2h\beta c_A^t c_V^t)\sin^2\theta\cos2\phi\Big\}\Big] \tag{11}$$

with $\beta = \sqrt{1-4m_t^2/s}$, and c_V^i, c_A^i as the couplings of Z to e^-e^+ and $t\bar{t}$. Explicitly, the couplings are:

$$c_V^e = \frac{1}{2\sin\theta_W\cos\theta_W}\Big(-\frac{1}{2} + 2\sin^2\theta_W\Big),$$
$$c_A^e = -\frac{1}{4\sin\theta_W\cos\theta_W},$$
$$c_V^t = \frac{1}{2\sin\theta_W\cos\theta_W}\Big(\frac{1}{2} - \frac{4}{3}\sin^2\theta_W\Big), \tag{12}$$
$$c_A^t = \frac{1}{4\sin\theta_W\cos\theta_W}.$$

In the above, h stands for the helicity of the top quark when the spin of the $\bar{t}$ is summed over, and for the negative of the helicity of the $\bar{t}$ when the spin of the top quark is summed over. The following may be noted: (a) the part of the distribution independent of the final state helicity was already given in Ref. [6] and that a sign error in the NP contributions therein is corrected here; and, (b) z' appears only in the NP contributions and is $+1$ for the top quark, and -1 for $\bar{t}$.

In order to render these expressions useful for ILC applications, and to disentangle the separate NP effects, we will define asymmetries that will isolate their individual contributions. These will be employed to obtain 90% confidence level limits on the NP couplings with realistic integrated luminosities in the absence of any signal at the ILC.

The explicit expressions in terms of the laboratory observables such as the momenta, polar, and azimuthal angles, accompanying the helicity independent and helicity dependent parts require a detailed discussion. Since the expressions above are quite involved, in order to get a better insight into the nature of the spin-momentum correlations and spin-spin correlations, in the Appendix we will consider a general framework first developed for a general inclusive process. This will enable us to interpret the angular correlations in terms of the vectorial quantities that define the process. Furthermore, it will also enable us to obtain insights into the symmetry properties of the correlations under the discrete symmetries C, P, and T and study the consequences of the CPT theorem.

IV. EXTRACTION OF NEW PHYSICS

In this section, we now address the question of isolating the contributions from the NP by constructing suitable asymmetries. Clever choices can lead to asymmetries receiving contributions from only one of them, while the others cancel out due to integrations over polar as well as azimuthal angles. Whereas in the helicity independent case it was impossible to disentangle the scalar and tensor contributions, now the rich structure of the helicity

dependent parts allows us to meet the objective that we have set out.

One may also ask to what extent this can be achieved if only one electron and positron spin configuration is available. Even in this case, it is possible to isolate the NP contribution term by term. Finally, we explore the situation when all spin configurations are available.

In this section, we have isolated the contributions coming from NP using different asymmetries. A thorough numerical analysis has been done to place constraints on the anomalous couplings.

A. Integrated asymmetries

For the case of angular distribution with transversely polarized beams, there is a dependence on the azimuthal angle. Compared to the unpolarized case, there are various terms with combinations such as $\sin\theta\cos\phi$, $\sin\theta\sin\phi$, $\sin\theta\cos\theta\sin\phi$, $\sin\theta\cos\theta\cos\phi$. We define below different azimuthal asymmetries which are used to isolate the couplings. The generic forms of the asymmetries, for the moment suppressing the beam polarizations, are:

$$A_1(\theta) = \frac{1}{\sigma^{\rm SM}(\theta)}\left[\int_0^{\pi}\frac{d\sigma_{\rm NP}}{d\Omega}d\phi - \int_{\pi}^{2\pi}\frac{d\sigma_{\rm NP}}{d\Omega}d\phi\right] \quad (13)$$

$$A_2(\theta) = \frac{1}{\sigma^{\rm SM}(\theta)}\left[\int_0^{(\pi/2)}\frac{d\sigma_{\rm NP}}{d\Omega}d\phi - \int_{\frac{\pi}{2}}^{(3\pi/2)}\frac{d\sigma_{\rm NP}}{d\Omega}d\phi + \int_{(3\pi/2)}^{2\pi}\frac{d\sigma_{\rm NP}}{d\Omega}d\phi\right] \quad (14)$$

where

$$\frac{d\sigma_{\rm NP}}{d\Omega} = \frac{d\sigma}{d\Omega}\bigg|_{h=1} - \frac{d\sigma}{d\Omega}\bigg|_{h=-1} \quad (15)$$

and

$$\sigma^{\rm SM}(\theta) = \left[\int_0^{2\pi}\frac{d\sigma_{\rm SM}}{d\Omega}d\phi\right]. \quad (16)$$

The above asymmetries amount to correlations between the spin direction of the top quark and its production angle. Expressed in a different language, they are azimuthal asymmetries calculated for the top polarization dependent part of the differential cross section.

$$\text{Case 1}: \begin{cases} A_1^{+-}(\theta) = \frac{1}{\sigma^{\rm SM}(\theta)}\frac{2m_t\alpha\beta\sin\theta}{\pi\sqrt{s}}\left[-2 + \frac{3s}{s-M_Z^2}(c_V^e c_V^t + \beta c_A^e c_A^t\cos\theta)\right]{\rm Im}T \\ A_2^{+-}(\theta) = \frac{1}{\sigma^{\rm SM}(\theta)}\frac{2m_t\alpha\beta\sin\theta}{\pi\sqrt{s}}\left[-1 + \frac{3s}{2(s-M_Z^2)}c_V^e c_V^t\right](2{\rm Re}T\beta\cos\theta - {\rm Re}S) \end{cases} \quad (17)$$

$$\text{Case 2}: \begin{cases} A_1^{++}(\theta) = \frac{1}{\sigma^{\rm SM}(\theta)}\frac{2m_t\alpha\beta\sin\theta}{\pi\sqrt{s}}\left[-1 + \frac{3s}{2(s-M_Z^2)}c_V^e c_V^t\right]({\rm Im}S - 2{\rm Im}T\beta\cos\theta) \\ A_2^{++}(\theta) = \frac{1}{\sigma^{\rm SM}(\theta)}\frac{2m_t\alpha\beta\sin\theta}{\pi\sqrt{s}}\left[2 - \frac{3s}{s-M_Z^2}(c_V^e c_V^t + \beta c_A^e c_A^t\cos\theta)\right]{\rm Re}T \end{cases} \quad (18)$$

The choice of our asymmetries can be justified by taking a close look at the expressions above. Confining ourselves to Case 1, it is seen that $A_1^{+-}(\theta)$ depends solely on ImT, whereas $A_2^{+-}(\theta)$ is proportional to both ReT and ReS. Similarly, for Case 2 the coupling ReT can be isolated from $A_2^{++}(\theta)$, whereas $A_1^{++}(\theta)$ is proportional to both ImS and ImT. Before proceeding further, we would like to point out that, when the final state helicity is summed over, only one asymmetry is nonzero for each beam-polarization combination [6]:

$$\text{Case 1: } \hat{A}_1^{+-}(\theta) = -\frac{1}{\sigma^{\rm SM}(\theta)}\frac{2m_t\alpha\beta\sin\theta}{\pi\sqrt{s}} \times\left[\frac{3}{2}\frac{s}{s-m_Z^2}c_A^e c_V^t\beta{\rm Im}\left(S + \frac{2c_A^t c_V^e}{c_V^t c_A^e}T\right)\right] \quad (19)$$

$$\text{Case 2: } \hat{A}_2^{++}(\theta) = \frac{1}{\sigma^{\rm SM}(\theta)}\frac{2m_t\alpha\beta\sin\theta}{\pi\sqrt{s}} \times\left[\frac{3}{2}\frac{s}{s-m_Z^2}c_A^e c_V^t\beta{\rm Re}\left(S + \frac{2c_A^t c_V^e}{c_V^t c_A^e}T\right)\right] \quad (20)$$

where

$$\hat{A}_1^{+-}(\theta) = \frac{1}{\sigma^{\rm SM}(\theta)}\left[\int_0^{\pi}\frac{d\sigma_{\rm tot}^{+-}}{d\Omega}d\phi - \int_{\pi}^{2\pi}\frac{d\sigma_{\rm tot}^{+-}}{d\Omega}d\phi\right] \quad (21)$$

$$\hat{A}_2^{++}(\theta) = \frac{1}{\sigma^{\rm SM}(\theta)}\left[\int_0^{(\pi/2)}\frac{d\sigma_{\rm tot}^{++}}{d\Omega}d\phi - \int_{(\pi/2)}^{(3\pi/2)}\frac{d\sigma_{\rm tot}^{++}}{d\Omega}d\phi + \int_{(3\pi/2)}^{2\pi}\frac{d\sigma_{\rm tot}^{++}}{d\Omega}d\phi\right] \quad (22)$$

and

$$\frac{d\sigma_{\rm tot}^{+\mp}}{d\Omega} = \frac{d\sigma^{+\mp}}{d\Omega}\Big|_{h=1} + \frac{d\sigma^{+\mp}}{d\Omega}\Big|_{h=-1} \tag{23}$$

The θ-integrated version of the asymmetries in Eqs. (13) and (14) is:

$$A_1(\theta_0) = \frac{1}{\Delta\sigma^{\rm SM}(\theta_0)}\Big[\int_{-\cos\theta_0}^{\cos\theta_0} \times \Big(\int_0^{\pi}\frac{d\sigma_{\rm NP}}{d\Omega}d\phi - \int_{\pi}^{2\pi}\frac{d\sigma_{\rm NP}}{d\Omega}d\phi\Big)d\cos\theta\Big] \tag{24}$$

where

$$\Delta\sigma^{\rm SM}(\theta_0) = \Big[\int_{-\cos\theta_0}^{\cos\theta_0}\Big(\int_0^{2\pi}\frac{d\sigma_{\rm SM}}{d\Omega}d\phi\Big)d\cos\theta\Big] \tag{25}$$

is independent of the transverse beam polarizations. $A_2(\theta_0)$ can be defined analogously to $A_1(\theta_0)$ above. A cutoff on θ has been introduced above, for a practical reason to stay away from the beam pipe. The asymmetries with the given limit on θ, $\theta_0 < \theta < \pi - \theta_0$, can be easily obtained. After the introduction of cutoff, the terms proportional to $\cos\theta$ vanish. Limiting ourselves to Case 1 we see that $A_1^{+-}(\theta_0)$ depends on ImT, and $A_2^{+-}(\theta_0)$ depends on ReS. It is seen that the coefficient of ImT in $A_1^{+-}(\theta_0)$ is twice that of ReS in $A_2^{+-}(\theta_0)$.

Continuing our analysis further, we note that we can determine only two of the four couplings, using either $++$ or $+-$ polarizations. For the determination of all of them, both polarization combinations have to be used. Restricting ourselves to the possibility that only one polarization combination is available, we can consider an additional asymmetry which combines a forward-backward asymmetry with an additional asymmetry in ϕ:

$$A_1^{\rm FB}(\theta_0) = \frac{1}{\Delta\sigma^{\rm SM}(\theta_0)}\Big[\int_0^{\cos\theta_0} d\cos\theta\Big(\int_0^{\pi}\frac{d\sigma_{\rm NP}}{d\Omega}d\phi - \int_{\pi}^{2\pi}\frac{d\sigma_{\rm NP}}{d\Omega}d\phi\Big) - \int_{-\cos\theta_0}^{0} d\cos\theta\Big(\int_0^{\pi}\frac{d\sigma_{\rm NP}}{d\Omega}d\phi - \int_{\pi}^{2\pi}\frac{d\sigma_{\rm NP}}{d\Omega}d\phi\Big)\Big] \tag{26}$$

$A_2^{\rm FB}(\theta_0)$ can be defined in an analogous way. These are easily evaluated for the $+-$ case:

$$A_1^{\rm FB}(\theta_0) = \frac{1}{\Delta\sigma^{\rm SM}(\theta_0)}\frac{4m_t\alpha\beta}{\pi\sqrt{s}}\Big[\frac{s}{s-M_Z^2}\beta c_A^e c_A^t\Big] \times (1-\sin^3\theta_0){\rm Im}T \tag{27}$$

$$A_2^{\rm FB}(\theta_0) = \frac{1}{\Delta\sigma^{\rm SM}(\theta_0)}\frac{4m_t\alpha\beta^2}{3\pi\sqrt{s}}\Big[-2+3\frac{s}{s-M_Z^2}c_V^e c_V^t\Big] \times (1-\sin^3\theta_0){\rm Re}T \tag{28}$$

The above expressions show $A_1^{\rm FB}(\theta_0)$ depends on ImT, and $A_1^{\rm FB}(\theta_0)$ is proportional to ReT. Thus all the couplings available for a single polarization combination can be isolated using the above asymmetries.

We have done a thorough numerical analysis in the next subsection for $+-$ case. The $++$ case can be treated analogously.

B. Numerical results

We have calculated the asymmetries under the ideal condition of 100% beam polarization for e^-, as well as e^+ at $\sqrt{s} = 500$ GeV and 800 GeV, respectively, for an integrated luminosity of 500 fb^{-1}. An explicit calculation has been done for the $(+-)$ case.

We first plot $A_1^{+-}(\theta)$ and $A_2^{+-}(\theta)$ in Fig. 1 and 2 as a function of θ for different center-of-mass (c.m.) energies. In Fig. 1, $A_1^{+-}(\theta)$ is plotted for Im$T = 0.01$ TeV^{-2}. Figure 2 shows $A_2^{+-}(\theta)$ which is a function of the anomalous couplings ReT and ReS, plotted as a function of θ with one coupling taken to be nonzero at a time. All the asymmetries here not only vanish for 0° and 180° because they are proportional to $\sin\theta$,, but $A_2^{+-}(\theta)$ for ReT also vanishes for 90° as it is additionally proportional to $\cos\theta$. The asymmetry $A_1^{+-}(\theta)$ can be as high as 9% in the future colliders for $\sqrt{s} = 800$ GeV, whereas $A_2^{+-}(\theta)$ can attain a maximum of 8% for ReT and 6% for ReS at the same c.m. energy, for the chosen values of the parameters as 0.01 TeV^{-2} each.

Figure 3 shows the θ integrated version of the asymmetries plotted as a function of the cutoff angle θ_0 for $\sqrt{s} = 500$ GeV and 800 GeV. Considering the $+-$ case, we find that $A_1^{+-}(\theta_0)$ depends only on ImT and $A_2^{+-}(\theta_0)$ depends only on ReS. For a value of 0.01 TeV^{-2} of the anomalous couplings, the asymmetries increase with the

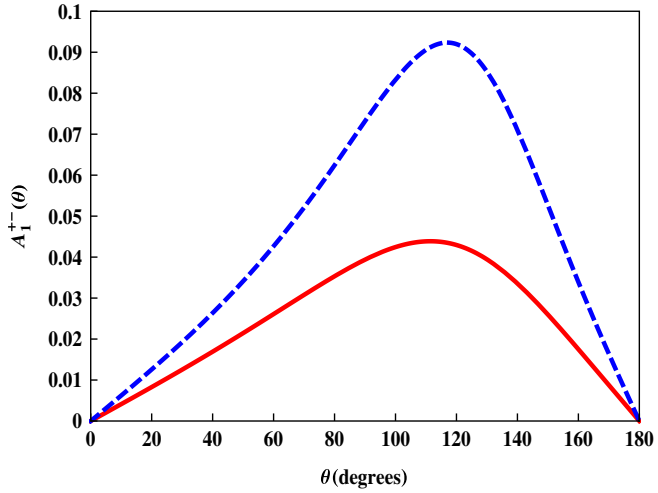

FIG. 1 (color online). $A_1^{+-}(\theta)$ as a function of θ for a value of Im$T = 0.01$ TeV^{-2} at $\sqrt{s} = 500$ GeV [Red-Solid line] and $\sqrt{s} = 800$ GeV [Blue-Dashed line].

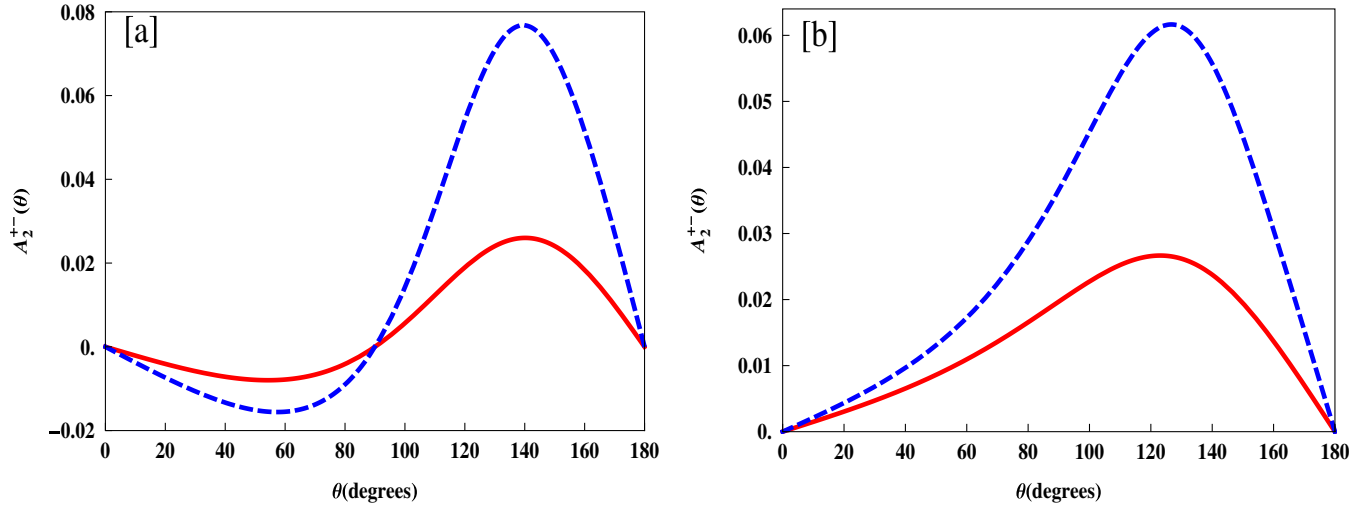

FIG. 2 (color online). $A_2^{+-}(\theta)$ as a function of θ for [a] Re$T = 0.01$ TeV^{-2}, Re$S = 0$, [b] Re$S = 0.01$ TeV^{-2}, Re$T = 0$ at $\sqrt{s} = 500$ GeV [Red-Solid line] and $\sqrt{s} = 800$ GeV [Blue-Dashed line].

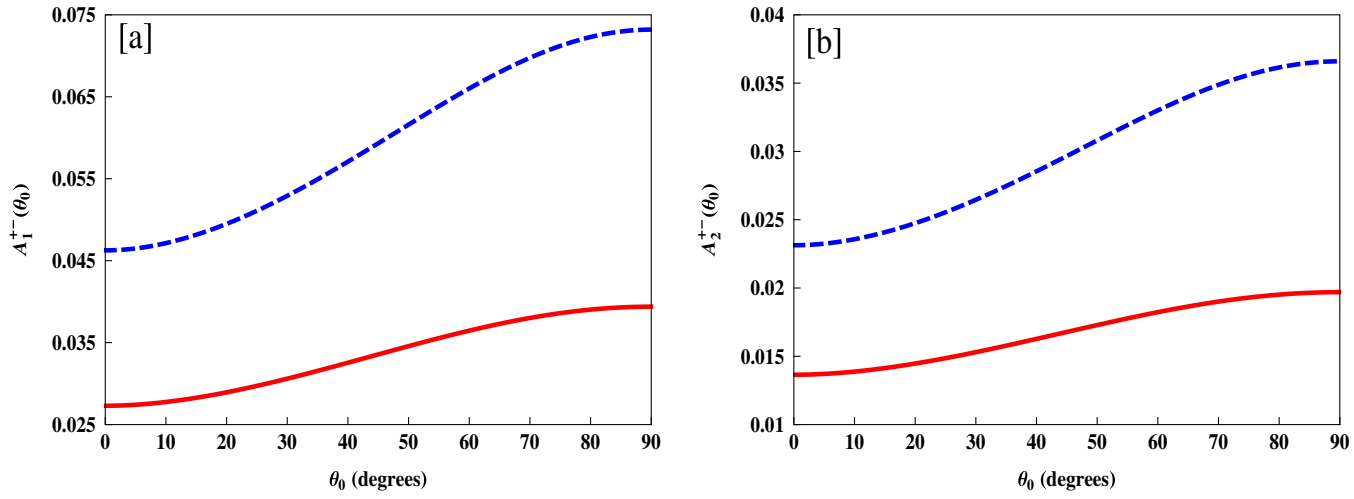

FIG. 3 (color online). The asymmetries as a function of θ_0 for $\sqrt{s} = 500$ GeV [Red-Solid line] and $\sqrt{s} = 800$ GeV [Blue-Dashed line] for [a] Im$T = 0.01$ TeV^{-2} of $A_1^{+-}(\theta_0)$ [b] Re$S = 0.01$ TeV^{-2} of $A_2^{+-}(\theta_0)$.

cutoff in both cases. This is due to the SM cross section in the denominator $\sigma^{\rm SM}(\theta_0)$ which decreases faster than the numerator. As is clear from Fig. 3, the asymmetries are sensitive to the c.m. energy even in the θ-integrated case.

Since we are trying to utilize a single beam-polarization combination for the isolation of the couplings as far as possible, we move to the next θ integrated forward-backward asymmetry $A_1^{\rm FB}(\theta_0)$ and $A_2^{\rm FB}(\theta_0)$ for the $+-$ case. $A_1^{\rm FB}(\theta_0)$ depends on ImT as in $A_1^{+-}(\theta_0)$. Figure 4(a) shows $A_1^{\rm FB}(\theta_0)$ plotted as a function of cutoff for Im$T = 0.01$ TeV^{-2}. The asymmetry here is much smaller than Fig. 3(a) for same value of ImT. This is due to the presence of the term $\beta c_A^e c_A^t$ before ImT in $A_1^{\rm FB}(\theta_0)$, which is much smaller than the term accompanying ImT in $A_1(\theta_0)$. The term in the later case is $(-2 + 3c_V^e c_V^t s/(s - M_Z^2))$. Figure 4(b) shows $A_2^{\rm FB}(\theta_0)$ plotted for Re$T = 0.01$ TeV^{-2}. Both the asymmetries here vanish for $\theta = 90°$ due to the $(1 - \sin^3\theta_0)$ term in the numerator.

We have used the asymmetries to calculate 90% CL limits that can be obtained with ILC, with an integrated luminosity $\mathcal{L}$ of 500 fb^{-1}, and $\sqrt{s} = 500$ GeV and 800 GeV. The sensitivity of the given coupling denoted by $\mathcal{C}_{\rm limit}$ is related to the value A of the asymmetry by:

$$\mathcal{C}_{\rm limit} = \frac{1.64}{|A|\sqrt{N_{\rm SM}}} \tag{29}$$

where $N_{\rm SM}$ is the number of SM events. The coefficient 1.64 may be obtained from statistical tables for hypothesis testing with one estimator.

Figure 5 shows the 90% CL limits obtained on ImT and ReS from $A_1^{+-}(\theta_0)$ and $A_2^{+-}(\theta_0)$, respectively. It is seen from the figures that the limits are relatively insensitive to

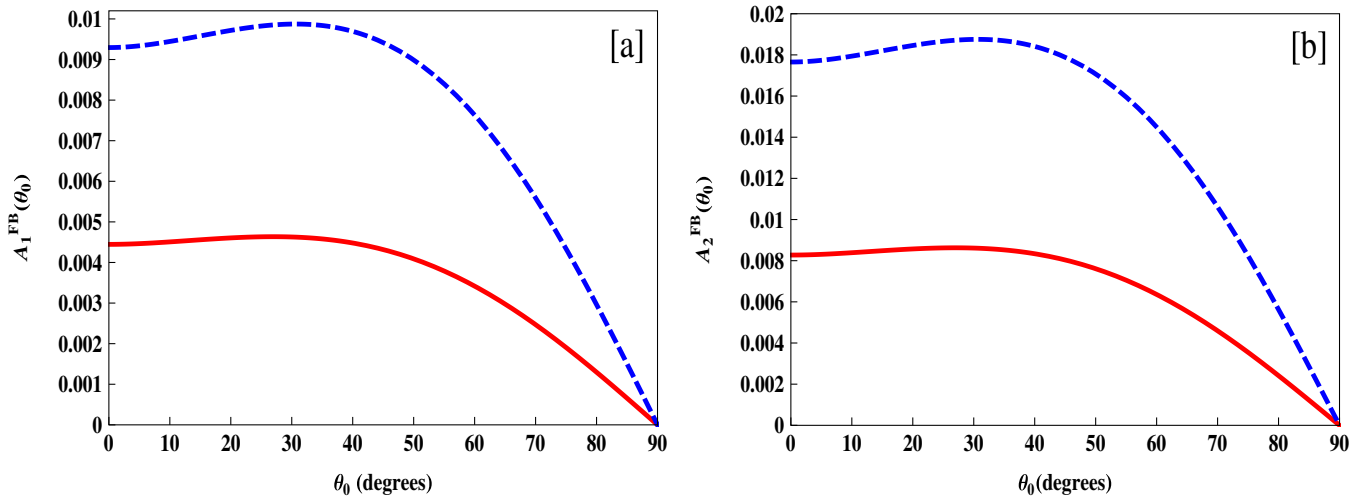

FIG. 4 (color online). The asymmetries as a function of θ_0 for $\sqrt{s} = 500$ GeV [Red-Solid line] and $\sqrt{s} = 800$ GeV [Blue-Dashed line] for [a] Im$T = 0.01$ TeV^{-2} of $A_1^{\rm FB}(\theta_0)$ [b] Re$T = 0.01$ TeV^{-2} of $A_2^{\rm FB}(\theta_0)$ for $+-$ case.

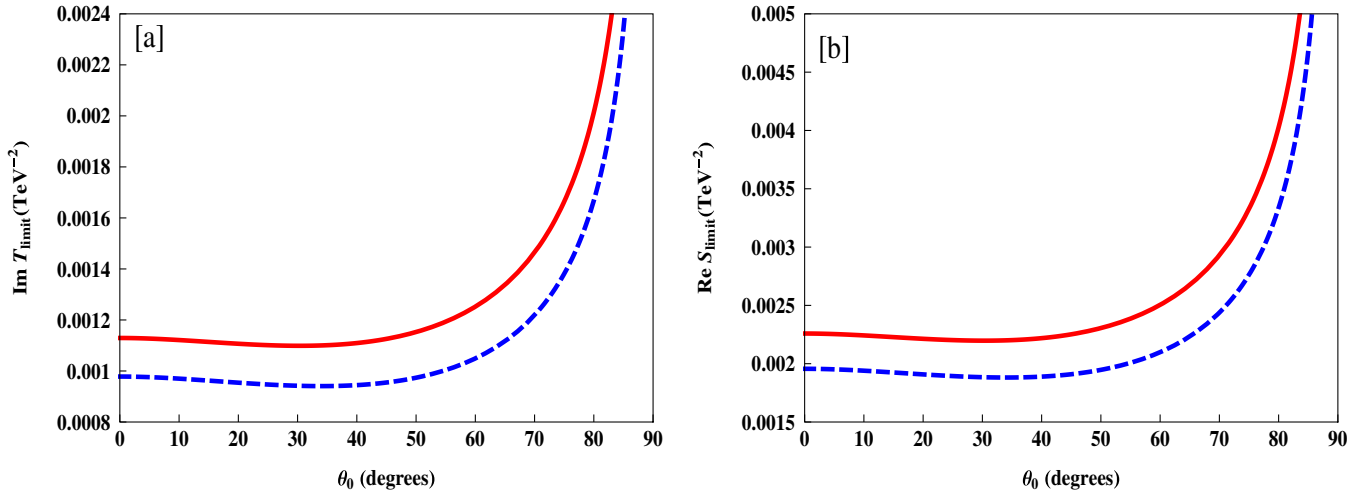

FIG. 5 (color online). 90% CL limit obtained on [a] ImT from $A_1^{+-}(\theta_0)$ [b] ReS from $A_2^{+-}(\theta_0)$ with an integrated luminosity of 500 fb^{-1} at $\sqrt{s} = 500$ GeV [Red-Solid line] and $\sqrt{s} = 800$ GeV [Blue-Dashed line] plotted as a function of θ_0.

the cutoff at very small values of θ_0. The best limit is obtained for about $\theta_0 = 40°$, though any nearby value of θ_0 will give similar results. The sensitivity corresponding to ImT is 1×10^{-3} TeV^{-2} (from $A_1^{+-}(\theta_0)$), and that corresponding to ReS is 2×10^{-3} TeV^{-2} (from $A_2^{+-}(\theta_0)$) at $\sqrt{s} = 800$ GeV, after which it increases rapidly. The results for the other couplings can be obtained in a straightforward manner. Considering $++$ and comparing it with $+-$, for $A_1^{+-}(\theta_0)$ and $A_2^{+-}(\theta_0)$, see Eqs. (17) and (18), the above sensitivities can be readily translated into sensitivities of other couplings. Comparing, we see ImS shares the same coefficient as ReS; furthermore, ReT and ImT also have the same coefficients. Therefore, the sensitivities in this case are the same as before; i.e. Im$T \leftrightarrow$ ReT and Re$S \leftrightarrow$ ImS, which are obtained by suitably interchanging the asymmetries $A_1(\theta_0) \leftrightarrow A_2(\theta_0)$.

Again, returning to the fact that only $+-$ case is utilized, then $A_2^{\rm FB}(\theta_0)$ can be used to put a limit on ReT. Figure 6 shows the behavior pattern is the same as before. Here, the limit obtained is about Re$T \sim 3.5 \times 10^{-3}$ TeV^{-2}. Compared to the above results, the limit obtained in this case is worse. Similarly $A_1^{\rm FB}(\theta_0)$ will give a limit on Im$T \sim 7 \times 10^{-3}$ TeV^{-2}, which is worse than the previous limit obtained from $A_1^{+-}(\theta_0)$. The limits obtained on the various couplings is summarized in Table I.

We point out that, when the top spin is not considered, the 90% CL limit on the imaginary part of Eq. (1) is 1.6×10^{-2} TeV^{-2}, from [6]. In Eq. (1), keeping the value of S and T to be nonzero one at a time, the limit on ImS is 1.6×10^{-2} TeV^{-2} and that on ImT is 4.4×10^{-2} TeV^{-2} at $\sqrt{s} = 500$ GeV, for an integrated luminosity of 500 fb^{-1}. Comparing this result with the one obtained

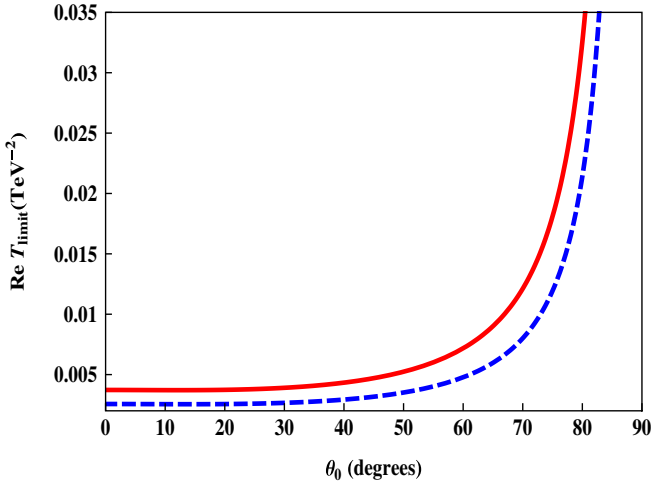

FIG. 6 (color online). 90 % CL limit obtained on ReT from $A_2^{\rm FB}(\theta_0)$ for $+-$ case with an integrated luminosity of 500 fb^{-1} at $\sqrt{s} = 500$ GeV [Red-Solid line] and $\sqrt{s} = 800$ GeV [Blue-Dashed line] plotted as a function of θ_0.

for $\sqrt{s} = 500$ GeV, considering the top spin, the sensitivities obtained are Im$S \sim 2.3 \times 10^{-3}$ TeV^{-2} and Im$T \sim 1.2 \times 10^{-3}$ TeV^{-2} from $A_1^{++}(\theta_0)$ and $A_1^{+-}(\theta_0)$, respectively. The limits in this case are an order of magnitude better than the previous one [6].

V. SELECTING A SAMPLE OF POLARIZED TOP QUARKS

In the above, we implicitly assume that it would be possible to isolate a sample of events where the top (and antitop) has a definite helicity. However, in practice, this is not possible as one can only measure polarization at a statistical level. Unlike an incoming beam of particles, which can be prepared in a pure spin state, an outgoing particle is not available in a pure state, but only a mixed state, yielding only an average polarization. In order to be able to make use of the definitions of various asymmetries which we discuss, we propose a practical method which would serve to provide a sample with predominantly positive or negative top helicities. This would of course lead to a depletion of the efficiency, but would be able to achieve the main objective. In the rest frame of the top, the angular distribution of a given decay product is given by,

$$\frac{1}{\Gamma}\frac{d\Gamma}{d\cos\Theta} = \frac{1}{2}(1 + P_t \kappa \cos\Theta) \tag{30}$$

where Θ is the angle between the momentum of the decay product and top-spin quantization axis, which is also the direction of the top momentum before a boost to the rest frame, P_t is the top polarization (longitudinal), and κ is the analyzing power for that decay channel. For a charged-lepton, κ is 1, giving the maximum analyzing power. Thus, if the top rest frame is constructed event by event, and the event then classified depending on whether cosΘ is positive or negative, we would have two event samples, one with dominantly positive helicity tops, and the other with dominantly negative helicity tops. The relative sizes of the two samples will depend on the actual polarization for that particular top (i.e. the top emitted at definite angles Θ_t, ϕ_t in the lab frame). The observables which we use are defined with respect to $d\sigma_{\rm NP}/d\Omega$, and the number of events in the difference of these two samples for a particular Θ_t and ϕ_t (of the top) would be proportional to this $d\sigma_{\rm NP}/d\Omega$, though not its actual value.

To use this method completely, one has to actually generate events including top decay, use our formulas to make predictions, and then compare the expected number of events for a given set of anomalous couplings with experiment and hence put a limit. Such a procedure would give limits which are less stringent than obtained in our analysis. Strictly speaking we should include full spin density matrices for t (or $\bar{t}$) production as well as decay into a certain final state, and consider asymmetries constructed out of the momenta of the decay products. However, we expect that the procedure described here

TABLE I. 90% CL limit obtained on the coupling along with the relevant asymmetries given for the cases of $+-$ and $++$ case.

$\sqrt{s}$	Case	Coupling	Individual limit from asymmetries			
			$A_1(\theta_0)$	$A_2(\theta_0)$	$A_1^{\rm FB}(\theta_0)$	$A_2^{\rm FB}(\theta_0)$
500 GeV	$+-$	ReS	2.3×10^{-3} TeV^{-2}			
		ReT				5.2×10^{-3} TeV^{-2}
		ImT	1.2×10^{-3} TeV^{-2}		1.0×10^{-2} TeV^{-2}	
		ImS	2.3×10^{-3} TeV^{-2}			
	$++$	ReT		1.2×10^{-3} TeV^{-2}		1.0×10^{-2} TeV^{-2}
		ImT			5.2×10^{-3} TeV^{-2}	
800 GeV	$+-$	ReS	2.0×10^{-3} TeV^{-2}			
		ReT				3.5×10^{-3} TeV^{-2}
		ImT	1.0×10^{-3} TeV^{-2}		7×10^{-3} TeV^{-2}	
		ImS	2.0×10^{-3} TeV^{-2}			
	$++$	ReT		1.0×10^{-3} TeV^{-2}		7×10^{-3} TeV^{-2}
		ImT			3.5×10^{-3} TeV^{-2}	

will approximate such a complete description, with some reduction of efficiency.

A full analysis including top decay entails a more complicated analysis with a different final state, and is beyond the scope of this work.

A similar procedure has been described in the context of τ polarization [18], where a suggestion is made for applying a cut on the energy fraction of the decay product of τ as a filter for τ polarization. The same technique of applying cuts on the energy fraction of a top decay product would be equivalent to that of applying a cut on $\cos\Theta$ that we have suggested above.

VI. DISCUSSION AND CONCLUSIONS

To conclude, in this paper we have considered the process $t\bar{t}$ in the presence of NP contributions due to scalar and tensor interactions, accounting for these at leading order only. Because of chirality conservation due to the near masslessness of the electron, these can be manifested only in the presence of TP. In contrast to earlier studies of this process, we have explicitly looked at the analysis of this process due to top-quark spin. The immediate advantage of this even when the spin of the $\bar{t}$ is summed over is that it now becomes possible to disentangle the contributions of S and T, which was not possible when no final state spin was measured. We have explicitly presented the differential cross sections, in as compact a manner as possible, where it is possible also to interchange the role of the spins of the t and $\bar{t}$.

In principle, it is also possible to consider the cases where the helicities of the top as well as the antitop are also explicitly resolved. It may be possible to carry out a study based on this, but is beyond the scope of the present work, as the features that we wish to study are already apparent when we sum over the helicity of one of the other. Furthermore, measuring both spins would lead to a loss in statistics thereby making this option less attractive.

We have then carried out an extensive numerical analysis based on these cross sections by defining suitable integrated asymmetries. By employing realistic integrated luminosity we have obtained 90% CL limits that can be placed on the NP couplings. With an integrated luminosity of 500 fb^{-1} and realistic beam polarizations, the limits on real and imaginary parts for T and S are of order 10^{-3} TeV^{-2} at $\sqrt{s} = 500$ and 800 GeV. These limits are found to be better by an order of magnitude compared to the previous case. These thus fare better than the corresponding analysis based on only momentum measurements when the spins of both final state particles are summed over. It is also of interest to compare these numbers with the naturalness constraints $O(10^{-3})$ TeV^{-2} on ReT from the $g-2$ of the electron, which is the most stringent one, whereas weaker constraints exist on the corresponding imaginary part from the electron electric dipole moment, see Ref. [6].

We have assumed in this work perfect beam polarization. If we were to take as in Ref. [6] $P_e = 0.8$ and $P_{\bar{e}} = -0.7$, then once again we would lose a factor of ≈ 0.7 in the asymmetry with a corresponding lowering of sensitivity. It must, however, be mentioned that one cannot directly isolate events with top helicities of $+1$ or -1. Hence to measure the asymmetries we discuss, one would have to carry out a subtraction of events in two kinematic regions of the decay products corresponding to positive and negative polarizations of the top. Doing so would entail a loss of efficiency to a certain extent. We have not taken this into account.

In order to understand the nature of the spin-momentum and spin-spin correlations, we have made contact with the general inclusive formalism developed in refs. [10,11]. This has required us to explicitly spell out the spin vector for the top quark and to identify the spin structure functions. Interestingly, ReS induces only one type of spin structure function, while ReT induces three types of spin structure functions. Analogous statements hold for the imaginary parts as well. The advantage of this formalism is that one is able to explicitly study the properties of the correlations under the discrete symmetries C, P, and T. Our discussion is more explicit than the discussion in the context of the inclusive process in Ref. [12]. It must be emphasized that to comprehend the structure of the spin-momentum correlations and the discrete symmetry properties of each of the terms in the distributions without this framework would be nearly impossible. This discussion is presented in the Appendix.

Finally, it must also be mentioned here that the process under consideration is of interest in the context of electroweak Sudakov processes with TP, see e.g. Ref. [19]. It would be interesting to actually carry out a study to see how these effects could mimic effects arising from NP of this type. This could be the topic of a future study.

ACKNOWLEDGMENTS

B. A. thanks the Homi Bhabha Fellowships Council for support. S. D. R. thanks the Theory Group of TIFR Mumbai, where part of this work was done, for hospitality.

APPENDIX: INTERPRETATION IN THE GENERAL INCLUSIVE FRAMEWORK

As mentioned in the Introduction, one of the main reasons for considering TP for at least one of the beams is that NP of the S and T type will not otherwise appear in distributions at linear order. This feature, a result of chirality conservation in the limit of massless electrons, is also the cornerstone of the analysis for a general inclusive process recently considered in the context of the ILC in refs. [10,11]. In spirit, this approach of retaining NP at linear order follows the one proposed in the context of neutral currents by Dass and Ross (DR) [12,20].

The outcome of this approach is that the spin-momentum correlations involving the incoming particles and the momentum of the observed particle, or the momenta of the two observed particles uniquely fingerprints the Lorentz structure of the NP. The approach here is fruitful in many ways. For instance, it was concluded that no CP violating couplings of the type V and A would show up in the inclusive process $e^+e^- \to h(p)X$ via spin-momentum correlations if NP amplitude were to interfere with QED contribution to the SM amplitude. This conclusion also remained true for the $Z-$ contribution to the SM amplitude as well, which was explicitly demonstrated in Ref. [10]. In processes such as the above, the physics would be described entirely in terms of ''momentum structure functions''. Note that whereas in Ref. [12], the spin and momentum of one observed particle was also considered, this has not been done in the context of ILC physics. The general inclusive framework is described in terms of ''structure functions'' associated with the inclusive final state, one for each type of interaction as well as for the various vectors from which Lorentz invariant amplitudes were constructed, when contracted with the leptonic tensor built out of the interference of the SM and NP diagrams, essential features of which will be recalled below.

Here we provide a concrete illustration for the case of the observed particle being the top quark, *viz.* a spin-1/2 particle, with the task at hand now being the identification of what will be called the ''spin structure functions''. The objective now is to relate the general inclusive framework to that of the computed distributions for the explicit $t\bar{t}$ final state, which explicitly receive contributions that are spin-independent and those that are not, and the latter expressed in a straightforward manner on h.

The correspondence to the framework for the helicity independent part of the correlations that appears in the process represented by Eq. (2) has already been done and presented in [10]. This correspondence was straightforward and no detailed discussion was presented. For the helicity dependent part, however, the correspondence is more involved and it is worth presenting a detailed discussion.

1. Formalism for the spin-momentum correlations

To begin the discussion, we begin by observing that the spin-momentum correlations amongst those of the incoming particles and the outgoing particles will arise from the interference between the SM currents with the NP ''currents'' which requires us to consider the trace:

$$\mathrm{Tr}[(1 - \gamma_5 h_+ + \gamma_5 \not{s}_+)\not{p}_+ \gamma_\mu (g_V^e - g_A^e \gamma_5) \times (1 + \gamma_5 h_- + \gamma_5 \not{s}_-)\not{p}_- \Gamma_i] H^{i\mu}. \tag{A1}$$

following the notation of Refs. [10,11], where i now is a generic index that denotes the scalar, pseudoscalar and tensor interactions, $h_\pm$ are the degrees of longitudinal polarization, and $s_\pm$ represent the transverse polarizations of the positron and electron. In terms of the scalar, pseudoscalar and tensor couplings g_S, g_P, and g_T of the electron, and structure functions describing the inclusive process given by F^r, F_1^{rut}, F_2^r, PF_1^{rut} and PF_2^r, we may express the vertices Γ_i and $H^{i\mu}$ as

$$\Gamma = g_s + i g_p \gamma_5 \tag{A2}$$

and

$$H_\mu^S = \left(r_\mu - q_\mu \frac{r \cdot q}{q^2}\right) F^r, \tag{A3}$$

where r is p_t, s_t or $n(n_\mu \equiv \epsilon_{\mu\alpha\beta\gamma} p_t^\alpha s_t^\beta q^\gamma)$, for S and P type NP interactions, and

$$\Gamma_{\rho\tau} = g_T \sigma_{\rho\tau}. \tag{A4}$$

$$H_{\mu\rho\tau}^T = (r_\rho u_\tau - r_\tau u_\rho) t_\mu F_1^{\mathrm{rut}} + (g_{\rho\mu} r_\tau - g_{\tau\mu} r_\rho) F_2^r + \epsilon_{\rho\tau\alpha\beta} r^\alpha u^\beta t_\mu P F_1^{\mathrm{rut}} + \epsilon_{\rho\tau\mu\alpha} r^\alpha P F_2^r \tag{A5}$$

where r is q, p_t, or s_t. Similarly u is chosen to be one of q, p_t, s_t, or n and t being p_t, s_t, or n respectively for T type interactions. [1] One may then evaluate the spin-momentum correlations due to the various structure functions in a straightforward manner. For ease of comparison, one may also compare against spin-momentum correlations that are tabulated in the appropriate tables in Ref. [11]. In terms of the kinematic quantities suitable to the process, which are $\vec{K} \equiv (\vec{p}_- - \vec{p}_+)/2 = E\hat{z}$, $q \equiv p_- + p_+$ with $q^0 = 2E$ and $\vec{q} = 0$. The analysis may be readily extended to the case of spin-momentum and spin-spin (helicity) correlations, where the latter is that of the observed final state particle.

In order to achieve this end, we first require an explicit representation for the vector describing the spin of the observed particle, s_t. In the helicity eigenbasis, the components of the spin vector s_t are (see, e.g., Eq. (3.155) in Ref. [21])

$$(|\vec{p}_t|/m_t, E\vec{p}_t/(m_t|\vec{p}_t|)). \tag{A6}$$

This representation for the spin vector in the helicity basis follows from considering free spinors for the quark and antiquark, first in their respective rest frames and then boosting them to the laboratory frame. By considering covariant generalization of the appropriate Pauli matrices to define the spin and introducing spin projection operator and choosing the spin direction to be that of the momentum, which is the appropriate choice for the helicity basis

[1] The structure functions for the case of the process given by Eq. (2) appear with no superscripts as there is only one vector p, the momentum of the observed particle, on hand. By straightforward inspection it was inferred in Ref. [10] that a correspondence between the inclusive process and $t\bar{t}$ production could be inferred: the correspondence was given as the structure functions $\mathrm{Re}(g_P F)$ and $\mathrm{Re}(g_T F_2)$ as arising from $\mathrm{Im}S_{RR}$ and $\mathrm{Im}T_{RR}$.

TABLE II. Structure functions along with the correlation in vector and polar form for the $++$ case and coupling which give rise to the structure functions.

Structure function	Correlation		Coupling
	Vector form	Polar form	
$\mathrm{Re}(g_T P F_2^{s_t})$	$4E^2 \vec{s}_t \cdot (\vec{s}_+ + \vec{s}_-)$	$\frac{4E^3}{m_t} g_V^e \sin\theta \cos\phi$	ReT
$\mathrm{Re}(g_T F_1^{p_t q s_t})$	$4E(E[p_t^0(\vec{q} \times \vec{s}_t^T) - q^0(\vec{p}_t \times \vec{s}_t^T]\cdot (\vec{s}_+ + \vec{s}_-) + [(\vec{p}_t \times \vec{q}) \cdot \vec{p}_+]\vec{s}_t \cdot (\vec{s}_+ - \vec{s}_-))$	$\frac{8E^4}{m_t} \lvert\vec{p}_t\rvert g_V^e \sin\theta \cos\theta \sin\phi$	ImT
$\mathrm{Im}(g_T F_1^{p_t q s_t})$	$4E^2([(\vec{p}_t^T \cdot \vec{s}_t^T)\vec{q} - (\vec{q}^T \cdot \vec{s}_t^T)\vec{p}_t]\cdot (\vec{s}_+ - \vec{s}_-) + (q^0 p_t^3 - q^3 p_t^0)\vec{s}_t \cdot (\vec{s}_+ - \vec{s}_-))$	$\frac{8E^4}{m_t} \lvert\vec{p}_t\rvert g_A^e \sin\theta \cos\theta \cos\phi$	ReT

we obtain the desired expression. With this explicit representation and with the identification of the vector $\vec{r}$ as $\vec{s}_t$, one may now turn to the appropriate tables in Ref. [11].

Consider now the case of $++$ (we introduce a notation $ij, i, j = +, -$ to denote the sense of the polarization of the electron (i) and positron (j), respectively). We may now compute the correlation directly, or we need simply to look at the correlation due to the structure function $\mathrm{Im}(g_s F^{s_t})$ which from Table 1 of Ref. [11] reads:

$$2E g_V^e \vec{K} \cdot (\vec{s}_+ + \vec{s}_-) \times \vec{s}_t. \tag{A7}$$

The above evaluates in terms of the kinematics of the reaction at hand to

$$\frac{2E^3}{m_t} g_V^e \sin\theta \sin\phi. \tag{A8}$$

Now looking into the explicit expression for the distribution for $t\bar{t}$ production, Eq. (9), one may readily see that the same angular dependence of this correlation is the one that accompanies ImS. Stated differently, the four-fermion contact interaction due to ImS induces the structure function $\mathrm{Im}(g_s F^{s_t})$. This completes the first correspondence that we are after.

This analysis may now be extended to the four-fermion contact interactions due to T. This interaction induces more than one kind of structure function, which can be explicitly obtained. It turns out that there are three such structure functions, which are presented with the respective correlations read off from Table 3 of Ref. [11], and the corresponding expressions in terms of the present kinematics as well as the four-fermion interactions which are responsible for inducing the relevant structure functions are shown in Table II.

Turning to the case of $+-$, we now consider the analogous correlations. In case of the scalar, the structure function $\mathrm{Im}(g_p f^{s_t})$ generates (see Table 1 of Ref. [11]) the correlations

$$-2E^2(\vec{s}_+ - \vec{s}_-) \cdot \vec{s}_t \tag{A9}$$

which evaluates to

$$-\frac{2E^3}{m_t} g_V^e \sin\theta \cos\phi. \tag{A10}$$

It may be readily seen by inspecting Eq. (10), this structure function is generated by the four-fermion interaction due to ReS.

The tensor part gives rise to three structure functions which are presented in Table III. The corresponding correlations are read off from Table 3 of Ref. [11], and the explicit representation in terms of the kinematics of the present process are also tabulated, as well as the NP terms that induce these structure functions.

In summary, we have presented here in detail the generalization of the result in Ref. [10] for the momentum structure function to the spin structure functions induced by the four-Fermi interactions. These results are helpful in understanding the C (charge conjugation), P (parity), and T (time-reversal) properties of the correlations which is the subject of the forthcoming subsection.

TABLE III. Structure functions along with the correlation in vector and polar form for the $+-$ case and coupling which give rise to the structure functions.

Structure function	Correlation		Coupling
	Vector form	Polar form	
$\mathrm{Re}(g_T F_2^{s_t})$	$-4E(\vec{s}_+ - \vec{s}_-) \times \vec{K} \cdot \vec{s}_t$	$-\frac{4E^3}{m_t} g_V^e \sin\theta \sin\phi$	ImT
$\mathrm{Re}(g_T P F_1^{p_t q s_t})$	$4E^2([(\vec{p}_t^T \cdot \vec{s}_t^T)\vec{q} - (\vec{q}^T \cdot \vec{s}_t^T)\vec{p}_t]\cdot (\vec{s}_+ + \vec{s}_-) + (q^3 p_t^0 - q^0 p_t^3)\vec{s}_t \cdot (\vec{s}_+ - \vec{s}_-))$	$-\frac{8E^4}{m_t} \lvert\vec{p}_t\rvert g_V^e \sin\theta \cos\theta \cos\phi$	ReT
$\mathrm{Im}(g_T P F_1^{p_t q s_t})$	$4E(E[p_t^0(\vec{q} \times \vec{s}_t^T) - q^0(\vec{p}_t \times \vec{s}_t^T]\cdot (\vec{s}_+ - \vec{s}_-) - [(\vec{q} \times \vec{p}_t) \cdot \vec{p}_+]\vec{s}_t \cdot (\vec{s}_+ + \vec{s}_-))$	$\frac{8E^4}{m_t} \lvert\vec{p}_t\rvert g_A^e \sin\theta \cos\theta \sin\phi$	ImT

TABLE IV. CP and T properties of different correlations appearing in the cross section for the reaction $e^-(p_-, s_-) + e^+(p_+, s_+) \to t(p_t, s_t) + \bar{t}(p_{\bar{t}}, s_{\bar{t}})$.

Case	NP Term	Correlation		CP	T
		Polar form	Vector form		
$++/--$	ReT	$\sin\theta\cos\phi$	$\frac{(\vec{s}_+ + \vec{s}_-)\cdot(\vec{p}_t - \vec{p}_{\bar{t}})}{\lvert\vec{p}_t - \vec{p}_{\bar{t}}\rvert}$	$+$	$+$
	ImS	$\sin\theta\sin\phi$	$\frac{(\vec{p}_- - \vec{p}_+)\times((\vec{s}_+ + \vec{s}_-)\cdot(\vec{p}_t - \vec{p}_{\bar{t}}))}{\lvert\vec{p}_- - \vec{p}_+\rvert\lvert\vec{p}_t - \vec{p}_{\bar{t}}\rvert}$	$+$	$-$
$+-/-+$	ReS	$\sin\theta\cos\phi$	$\frac{(\vec{s}_+ - \vec{s}_-)\cdot(\vec{p}_t - \vec{p}_{\bar{t}})}{\lvert\vec{p}_t - \vec{p}_{\bar{t}}\rvert}$	$-$	$+$
	ImT	$\sin\theta\sin\phi$	$\frac{(\vec{p}_- - \vec{p}_+)\times((\vec{s}_+ - \vec{s}_-)\cdot(\vec{p}_t - \vec{p}_{\bar{t}}))}{\lvert\vec{p}_- - \vec{p}_+\rvert\lvert\vec{p}_t - \vec{p}_{\bar{t}}\rvert}$	$-$	$-$

2. Properties under C, P, and T

A discussion on the properties of the correlations under the discrete symmetries of C, P, and T appearing in the distribution is the subject of this subsection. We note here that T will represent naïve time reversal, i.e. reversal of all spins and momenta, without interchange of initial and final states. We will see that the helicity dependent part of the correlations are substantially richer in structure compared to their helicity independent counterparts.

We begin by noting that the differential cross sections corresponding to antiparallel or parallel e^- and e^+ polarization have both CP-odd as well as CP-even quantities compared to the helicity independent parts. The additional features arise from the h and z' dependent quantities.

Let us keep in mind that at the level of the effective Lagrangian, if the projection operators are expanded out completely, and if the real and imaginary parts of S and T are separated, it can be checked that terms occurring with ReS and ReT are CP even, whereas the ones with ImS and ImT are CP odd. The question one may then ask is how this can be seen in the individual terms appearing in the distributions.

In order to achieve this end, the terms in the cross sections for the various spin configurations of the electron and positron spins have to be written in terms of the momentum and spin correlations which are explicitly even or odd. The requisite combinations are presented in Table IV.

The entries in Table IV enable us to decipher the CP properties in the following manner. Let us first note that the quantities h and hz' may be defined in the following manner:

$$h = \frac{(\vec{s}_t + \vec{s}_{\bar{t}}) \cdot (\vec{p}_t - \vec{p}_{\bar{t}})}{|\vec{p}_t - \vec{p}_{\bar{t}}|}, \tag{A11}$$

$$hz' = \frac{(\vec{s}_t - \vec{s}_{\bar{t}}) \cdot (\vec{p}_t - \vec{p}_{\bar{t}})}{|\vec{p}_t - \vec{p}_{\bar{t}}|}. \tag{A12}$$

Thus we may explicitly see that $CP(h) = +$, $T(h) = +$, and $CP(hz') = -$, $T(hz') = +$. From the expressions for the distributions, it can be checked considering the CP and T properties from the table, that the terms coming with ReS and ReT and those coming with ImS and ImT are both CPT even. This is due to the fact that the effective Lagrangian is Hermitian. As there are no non-Hermitian terms, there are no CPT odd terms, see Ref. [22].

Let us now consider the implications of this for the entries in Table IV with an explicit example. Consider the correlation in the distribution for the $++$ case accompanying ImS, which appears in the combination $hz' \sin\theta \sin\phi$, see Eq. (9). It may now be readily seen from Table IV that the term $\sin\theta \sin\phi$ is CP even and T odd, whereas hz' is CP odd and T even, and, as a result the entire term, is CP odd and CPT even. Analogous exercises may be carried for all the correlations appearing in the explicit differential cross sections.

Let us again emphasize that the top-helicity analysis allows us to isolate the T and S contributions for the following reasons: the four-Fermi interaction due to T gives rise to three different spin structure functions each with its characteristic spin-momentum correlation, whereas the one due to S gives rise to only one spin structure function. This is in contrast to the measurement with no top-spin analysis, where both T and S give rise to only one momentum structure function each, and also give rise to the same spin-momentum correlation, which is why we are unable to disentangle the contribution in this case. This gives to us an explicit understanding of these spin-momentum correlations, which one could not have obtained by merely inspecting the distributions. Secondly, without the present considerations we would not have been able to discuss the C, P, and T properties of the correlations.

Thus the general inclusive framework and the structure of the spin-momentum and spin-spin correlations provide a useful guide for understanding the properties of the correlations obtained in our exclusive process.

[1] G. Aarons *et al.* (ILC Collaboration), arXiv:0709.1893.
[2] E. Devetak and A. Nomerotski, arXiv:1005.1756.
[3] G. Moortgat-Pick *et al.*, Phys. Rep. **460**, 131 (2008).
[4] W. Buchmuller and D. Wyler, Nucl. Phys. B **268**, 621 (1986).
[5] B. Grzadkowski, Acta Phys. Pol. B **27**, 921 (1996) http://th-www.if.uj.edu.pl/acta/vol27/pdf/v27p0921.pdf.
[6] B. Ananthanarayan and S. D. Rindani, Phys. Rev. D **70**, 036005 (2004).
[7] A. Brandenburg, M. Flesch, and P. Uwer, Czech. J. Phys. **50**, 51 (2000).
[8] R. M. Godbole, S. D. Rindani, and R. K. Singh, J. High Energy Phys. 12 (2006) 021.
[9] K. i. Hikasa, Phys. Rev. D **33**, 3203 (1986).
[10] B. Ananthanarayan and S. D. Rindani, Eur. Phys. J. C **46**, 705 (2006).
[11] B. Ananthanarayan and S. D. Rindani, Eur. Phys. J. C **56**, 171 (2008).
[12] G. V. Dass and G. G. Ross, Nucl. Phys. B **118**, 284 (1977).
[13] B. Ananthanarayan, S. D. Rindani, R. K. Singh, and A. Bartl, Phys. Lett. B **593**, 95 (2004); **608**, 274(E) (2005).
[14] B. Ananthanarayan and S. D. Rindani, Phys. Lett. B **606**, 107 (2005).
[15] B. Ananthanarayan and S. D. Rindani, J. High Energy Phys. 10 (2005) 077.
[16] K. Rao and S. D. Rindani, Phys. Lett. B **642**, 85 (2006).
[17] K. Rao and S. D. Rindani, Phys. Rev. D **77**, 015009 (2008); **80**, 019901(E) (2009).
[18] M. Guchait and D. P. Roy, arXiv:0808.0438.
[19] P. Ciafaloni, D. Comelli, and A. Vergine, J. High Energy Phys. 07 (2004) 039.
[20] G. V. Dass and G. G. Ross, Phys. Lett. B **57**, 173 (1975).
[21] W. Greiner and J. Reinhardt, *Quantum Electrodynamics* (Springer-Verlag, Heidelberg, 2003), 3rd Ed..
[22] S. D. Rindani, Pramana **45**, 263 (1995).